Journal of Ginseng Research 47 (2023) 228–236

Contents lists available at ScienceDirect

Journal of Ginseng Research

journal homepage: https://www.sciencedirect.com/journal/journal-of-ginseng-research

Research Article

Integrative applications of network pharmacology and molecular docking: An herbal formula ameliorates H9c2 cells injury through pyroptosis

Zhongwen Qi [a, b, c], Zhipeng Yan [b, c, d], Yueyao Wang [b, c, d], Nan Ji [d], Xiaoya Yang [d], Ao Zhang [b], Meng Li [e, **], Fengqin Xu [a, ***], Junping Zhang [b, c, *]

[a] Postdoctoral Research Station of China Academy of Chinese Medical Sciences, Institute of Gerontology, Xiyuan Hospital, China Academy of Chinese Medical Sciences, Beijing, China
[b] First Teaching Hospital of Tianjin University of Traditional Chinese Medicine, Tianjin, China
[c] National Clinical Research Center for Chinese Medicine Acupuncture and Moxibustion, Tianjin, China
[d] Tianjin University of Traditional Chinese Medicine, Tianjin, China
[e] Institute of Hypertension, Jiangsu Province Hospital of Chinese Medicine, Affiliated Hospital of Nanjing University of Chinese Medicine, Nanjing, Jiangsu, China

ARTICLE INFO

Article history:
Received 28 December 2021
Received in revised form
23 February 2022
Accepted 17 March 2022
Available online 28 March 2022

Keywords:
Cardiomyocyte
Pyroptosis
Network pharmacology
Molecular docking
Ginsenoside

ABSTRACT

Background: QiShen YiQi pills (QSYQ) is a Traditional Chinese Medicine (TCM) formula, which has a significant effect on the treatment of patients with myocardial infarction (MI) in clinical practice. However, the molecular mechanism of QSYQ regulation pyroptosis after MI is still not fully known. Hence, this study was designed to reveal the mechanism of the active ingredient in QSYQ.
Methods: Integrated approach of network pharmacology and molecular docking, were conducted to screen active components and corresponding common target genes of QSYQ in intervening pyroptosis after MI. Subsequently, STRING and Cytoscape were applied to construct a PPI network, and obtain candidate active compounds. Molecular docking was performed to verify the binding ability of candidate components to pyroptosis proteins and oxygen-glucose deprivation (OGD) induced cardiomyocytes injuries were applied to explore the protective effect and mechanism of the candidate drug.
Results: Two drug-likeness compounds were preliminarily selected, and the binding capacity between Ginsenoside Rh2 (Rh2) and key target High Mobility Group Box 1 (HMGB1)was validated in the form of hydrogen bonding. 2 μM Rh2 prevented OGD-induced H9c2 death and reduced IL-18 and IL-1β levels, possibly by decreasing the activation of the NLRP3 inflammasome, inhibiting the expression of p12-caspase1, and attenuating the level of pyroptosis executive protein GSDMD-N.
Conclusions: We propose that Rh2 of QSYQ can protect myocardial cells partially by ameliorating pyroptosis, which seems to have a new insight regarding the therapeutic potential for MI.

1. Introduction

TCM has received wide attention recently in clinical major diseases. At the same time, its clinical promotion is limited, including the ambiguity of drug composition and treatment mechanism [1]. In recent years, the development of virtual screening network technology [2,3], which has brought opportunities for the study of active ingredients and specific mechanisms of TCM formula. The use of this biological information and virtual computing tools can more efficiently and accurately predict active ingredients and targets from TCM [4].

* Corresponding author. First Teaching Hospital of Tianjin University of Traditional Chinese Medicine, Tianjin, China.
** Corresponding author. Institute of Hypertension, Jiangsu Province Hospital of Chinese Medicine, Affiliated Hospital of Nanjing University of Chinese Medicine, Nanjing, Jiangsu, China.
*** Corresponding author. Postdoctoral Research Station of China Academy of Chinese Medical Sciences, Institute of Gerontology, Xiyuan Hospital, China Academy of Chinese Medical Sciences, Beijing, China.
E-mail addresses: zhongyilimeng@163.com (M. Li), Dr.xufengqin@outlook.com (F. Xu), tjzhtcm@163.com (J. Zhang).

https://doi.org/10.1016/j.jgr.2022.03.003

Molecular docking is a computational program that is used to identify the binding sites between drug proteins and macromolecular targets [5,6], initially to identify macromolecules and small molecules [7], and now is developed to assist drug discovery programs, such as drug repositioning, drug reverse screening, molecular repositioning, and other processes [8]. TCM formulas are difficult to identify due to the complexity of their active ingredients, and with the continuous improvement of molecular docking technology, the active ingredients in TCM formulas can be well predicted. Some researchers have selected efficient drug candidates of Chinese herbal compounds involved in tumor immune regulation and elucidated the potential basis in vivo and in vitro experiments [9]. Network pharmacology was first proposed in 2007 [10], which covers many links such as systems biology, network analysis, and biological information, and is an integration platform based on a comprehensive database to explain the relationship between TCM and diseases [11]. Collecting the active compounds of TCM formulas predicts of compounds-related targets by different databases, constructs a network diagram between herb-disease targets, maps the common target proteins between herb and diseases, then, performs network topology analysis of biological processes and signaling pathways for these targets, and finally validates the analysis results through different experiments. In conclusion, the intervention of network pharmacology can further predict the possible signaling pathways and biological processes. We previously clarified the possible links of Si-Miao-Yong-An Decoction (SMYAD), classic TCM formulas, treating cardiovascular disease by network pharmacology, and experimentally verified the possible mechanism by which SMYAD promotes the maturation of Vasa Vasorum to stabilize vulnerable plaques [12,13]. Therefore, the integrated application of network pharmacology and molecular docking can clarify the pharmacodynamic basis of TCM formulas, explain the compatibility of components and potential mechanism research, and more deeply understand the scientific connotation of multiple components and multiple targets of TCM.

QSYQ is a standardized Chinese herbal preparation (Approval number of CFDA: Z20030139) approved by the China Food and Drug Administration (CFDA) in 2003 [14], which consists of *Hedysarum Multijugum Maxim* (HM), *Radix Salviae* (SM), *Panax Notoginseng* (PN), and *Dalbergia Odorifera* (DO) at a proportion of 10:5:1:0.067 [15]. QSYQ is widely used in clinical practice for patients with cardiovascular disease of Qi deficiency and blood stasis syndrome, with significant clinical efficacy and safety [16]. Furthermore, we have previously shown that QSYQ can regulate energy metabolism, relieve ventricular remodeling and inhibit the inflammatory response after MI [17].

Pyroptosis is a programmed cell death mode different from apoptosis, which depends on the activation of aspartate-specific caspase-1 (caspase-1) [18]. Accumulating evidence suggests that the NLRP3-caspase-1 axis plays an important role in inflammation-induced cell death after MI [19]. Although QSYQ can inhibit the inflammatory response after MI [20], the specific active ingredient is unclear, and whether this active ingredient can relieve pyroptosis is also uncertain. In this study, we aimed to further screen the top candidate bioactive components of QSYQ in intervening pyroptosis after MI by network pharmacology and molecular docking comprehensive techniques, and to verify the protective effect of the candidate drugs on H9c2 cells by in vitro, providing value for the clinical indications of QSYQ and the candidate component drugs.

2. Materials and methods

2.1. Collection and screening of bioactive compounds in QSYQ

The main components of QSYQ: Huangqi (*Hedysarum Multijugum Maxim*, HM), Danshen (*Radix Salviae*, RS), Sanqi (*Panax Notoginseng*, PN), Jiangxiang (*Dalbergiae Odoriferae Lignum*, DO). All candidate herbal compounds of QSYQ were screened by use of TCMSP (http://tcmspnw.com/) [21], and the screening criteria were: relative molecular mass (MW) $\leq$ 500, oral bioavailability (OB) $\geq$ 50%, drug-likeness (DL) $\geq$ 0.1, and drug half-life (HL) $\geq$ 5. We screened the molecules of bioactive compounds with MW $\leq$ 500 to select the molecules that are easier to absorb and improve the efficacy of TCM. OB $\geq$ 50% have good absorption and slow metabolism after oral administration [22], DL $\geq$ 0.18 were chemically suitable for drug development [23].

2.2. Herb-compound-target network construction

The corresponding target genes of each active ingredient were searched in the TCMSP database. Use UniProt (https://www.uniprot.org/) database to convert all gene proteins into corresponding gene symbols with "*Homo sapiens*" species to standardize gene names and organisms [24], The resulting gene targets were intersected with the selected molecules of HM, RS, PN and DO and analyzed with Cytoscape (https://cytoscape.org/) to construct herb-compound-target networks [25].

2.3. Identification of pyroptosis-related targets and MI-related targets

Through GeneCards (https://www.genecards.org/) database to screen details associated with pyroptosis and MI [26], and only "*Homo sapiens*" genes linked to pyroptosis and MI were acquired. Subsequently, TCMSP and Cytoscape were mapped to the drug-compound-target network associated with pyroptosis and MI by using a Venny 2.1 online tool.

2.4. ADEM parameter analysis of top candidate drugs

The primary measure to evaluate the top candidate active compounds in the clinic is toxicokinetics (ADME), which mainly includes OB, DL, and HL. Due to the hemodynamic changes in patients with MI, resulting in reduced blood flow to organs, the drugs cannot be metabolized [27]. Therefore, the higher the OB amount, the lower the HL value, indicating the value of this component as a drug candidate.

2.5. Molecular docking to validate drug candidates

Whether the candidate ingredients initially screened can be used as a drug candidate is affected by the molecular binding ability to the target gene receptor [28]. In the PubChem database (https://pubchem.ncbi.nlm.nih.gov/), the compound were determined, and the 3D structure of the compound, constructed with Chem Office software, was used as a ligand molecule. Using the RCSB PDB (https://www.rcsb.org/) database to search the 3D structure of receptor molecules. MODELLER software was used to model and AutoDock Tools1.5.6 was applied to predict the binding energy of drug molecules and genes [29]. Possible binding sites of receptor to

ligand were recorded. If the binding energy is less than −5 kJ mol^{-1} [30]. Finally, the docking results of the observed compounds and proteins were analyzed using Pymol software.

2.6. H9c2 cells culture and OGD model construction

H9c2 cells were obtained from the Procell Life Science and Technology (Wuhan, China) and cultured in high-glucose (concentration 4.5 g/L) DMEM. Logarithmic phase H9c2 cells were collected and plated, then were placed in a cell incubator. The culture medium was changed to a serum-free and glucose-free DMEM, and the well plate was placed in the hypoxia chamber (Billups-Rothenberg, USA) to maintain the oxygen concentration at 1%. The cells were cultured for 12 h or 24 h with hypoxia.

2.7. H9c2 cells viability assay and Rh2 concentration screening

Logarithmic phase H9c2 cells were collected and adjusted to a density of 1×10^5/mL. The model was constructed according to the experimental groups. At the end of the intervention, H9c2 were added by 10 μL CCK-8 solution (Yeasen, Shanghai, China) for 3 h before further enzyme analyses (Tecan, German).

H9c2 cells were added with graded Rh2 (0.1–50 μM), operated according to the manufacturer's instructions of CCK8, and then select the optimal concentration of drug treatment.

2.8. Scanning electron microscopy observation of H9c2 cells

H9c2 cells were fixed with 2.5% glutaraldehyde (Servicebio, Wuhan, China) for 2 h, and then rinsed with 0.1% PBS three times, afterward, the samples were fixed in 1% osmic acid (Ted Pella, USA) for 2 h. Next, the samples were dehydrated through graded alcohols (30, 50, 70, 95, and 100%) and dried. Finally, the sketches were observed under a SU8100-HITACHI (Japan) scanning electron microscope (SEM) operating at 15 kV.

2.9. Measurement of IL-18 and IL-1β activities in cell supernatant

After the cells in each group were intervened, the cell supernatant was collected and centrifuged at 1200 g for 10 min to remove cell debris, IL-18 and IL-1β activities were measured using two activity assay kits (NeoBioscience, China), according to the manufacturer's instructions. Then their absorbance were detected at 450 nm by spectrophotometry (Tecan, German).

2.10. Western blot analysis

The expression of proteins associated with pyroptosis were measured by Western blot analysis with specific primary antibodies against NLRP3 (1:800), Caspase 1 (1:1000), GSDMD (1:500), IL-18 (1:1000), IL-1β (1:1000) and HMGB1 (1:500) (all from Abcam, UK).

2.11. Statistical analysis

Graph Pad Prism 8 statistical software was used for data analysis and processing. All results were represented as means ± standard deviation (SD) of at least three independent experiments. Student's t-test or one-way ANOVA test was used for statistical analyses of the difference between groups. P values < 0.05 were considered as significant.

3. Results

3.1. QSYQ-active compounds network analysis

By searching the TCMSP database, combined with characteristics: OB $\geq$ 50%, DL $\geq$ 0.1, and HL $\geq$ 5.35 active compounds were selected, contained in HQ, DS, SQ, and JX are 13, 5, 13, and 4, respectively. Basic information of active compounds in QSYQ (Table S1). The results suggest that the same active ingredients may exist in multiple herbs, and different herbs may contain multiple effective active ingredients, which also further provides material for the multi-target mechanism of TCM.

3.2. Herb-compound-target network construction in QSYQ

Convert all gene proteins through the UniProt database, 78 corresponding gene targets were obtained, and after removing duplicate targets, a total of 29 human-derived target proteins were obtained. The resulting common targets were intersected with the selected active compounds of HM, RS, PN, DO. In addition, an Herb-Compound-Target network VEEN map was constructed with Cytoscape (Fig. S1). This network consists of different nodes and edges, where nodes indicate herbs, active compounds, and compound-related targets, and edges represent interactions between active compounds and common target proteins. Among these targets, each target corresponds to a variety of active compounds, and each compound also has numerous targets, and finally acts together on 29 common target proteins. This suggests that the compounds in QSYQ may on these targets to exert pharmacological effects in myocardial protection.

3.3. Five Pyroptosis-MI common target proteins were screened by the GeneCards database

From the GeneCards database, 3548 genes related to MI and 98 genes related to pyroptosis were acquired. Subsequently, searched by the TCMSP database revealed that 110 of the 3548 genes were HM target genes, of which CASP1, HMGB1, PARP1, BCL2, and EGFR were genes associated with pyroptosis (Fig. S2A). There were 122 RS target genes and 107 PN target genes, all of which contained CASP1, HMGB1, PARP1, BCL2, and EGFR (Figs. S2B and C). But DO has only 30 target genes, of which only HMGB1 was associated with pyroptosis (Fig. S2D).

3.4. Seven top candidate compounds were selected by cytoscape mapping

Concerned with the TCMSP database get results, Cytoscape software was applied to construct a PPI network of therapeutic targets for QSYQ against MI and pyroptosis. OB $\geq$ 30% as the criterion, among the 43 components of HM, Qaempferol, and Quercetin could act directly on BCL2, EGFR, CASP1, and HMGB1 (Fig. S3A). Of the 105 components in RS, only Luteolin and Dehydrotanshinone IIA could impact BCL2, EGFR, CASP1, and HMGB1 (Fig. S3B). Of the 53 components in PN, only β-sitosterol, Ginsenoside Rh2, Quercetin, and Panaxydol could act directly on BCL2, EGFR, CASP1, and HMGB1 (Fig. S3C). Thus, it was figured out that in QSYQ, Quercetin, Kaempferol, Luteolin, Dehydrotanshinone IIA, β-sitosterol, Ginsenoside Rh2, and Panaxydol can influence pyroptosis by regulating the expression of BCL2, EGFR, CASP1, and HMGB1, which in turn makes the protective effect of MI.

3.5. Two drug-likeness compounds, β-sitosterol, and Rh2 were selected by ADEM parameters

Combined with different parameters of ADME (Table S2). Data analysis from the table showed that β-sitosterol and Rh2 had the highest DL values of 0.75 and 0.56, respectively. These results proposed that β-sitosterol and Rh2 were more likely to be acted as clinical medications. Additionally, the hemodynamics of patients with MI often change, resulting in reduced blood flow to organs, carrying out the inability of drugs to be metabolized. The DH of β-sitosterol and Rh2 was extremely short at 5.36 h and 11.08 h, respectively. Taking into account the hemodynamic characteristics of MI, it was highly recommended that β-sitosterol and Rh2 were more suitable as candidate drug-likeness compounds for the clinical treatment of MI.

3.6. Molecular docking was performed to verify the binding ability of Rh2 to target proteins

Through the construct PPI network, it was obtained that the common target protein of QSYQ-MI-pyroptosis was HMGB1, and the possible drug compounds were also analyzed. The hydrogen bonding ability of β-sitosterol and HMGB1 was much greater than −5.07 kcal/mol and formed an unstable complex. The binding energies, as well as the binding sites of Rh2 and HMGB1, were predicted by Autodock Tools1.5.6. The results demonstrated that Rh2 could bind to Lys 84, Lys 182, Glu 191, and Glu 72 of HMGB1 in the form of hydrogen bonding (total binding energy −5.07 kcal/mol) (Fig. S4).

3.7. The 12 h hypoxia model of OGD in H9c2 cells was efficient

To investigate the therapeutic effect of Rh2 on MI, the construction of the OGD model in vitro can properly simulate the pathological process of MI. However, there is no uniform standard for the duration of OGD hypoxia, and to determine the optimal construction time of the model, the cell morphology and survival were examined after hypoxia 12 h or 24 h of OGD, individually. The results presented that the morphology of H9c2 were basically intact at hypoxia 12 h, but the H9c2 were severely fragmented at hypoxia 24 h. Similarly, multiple pores were formed or even ruptured on the cell membrane surface, which was also consistent with the characteristics of pyroptosis injury, indicating that the pathological changes of pyroptosis occurred under the OGD (Fig. 1A and B). After

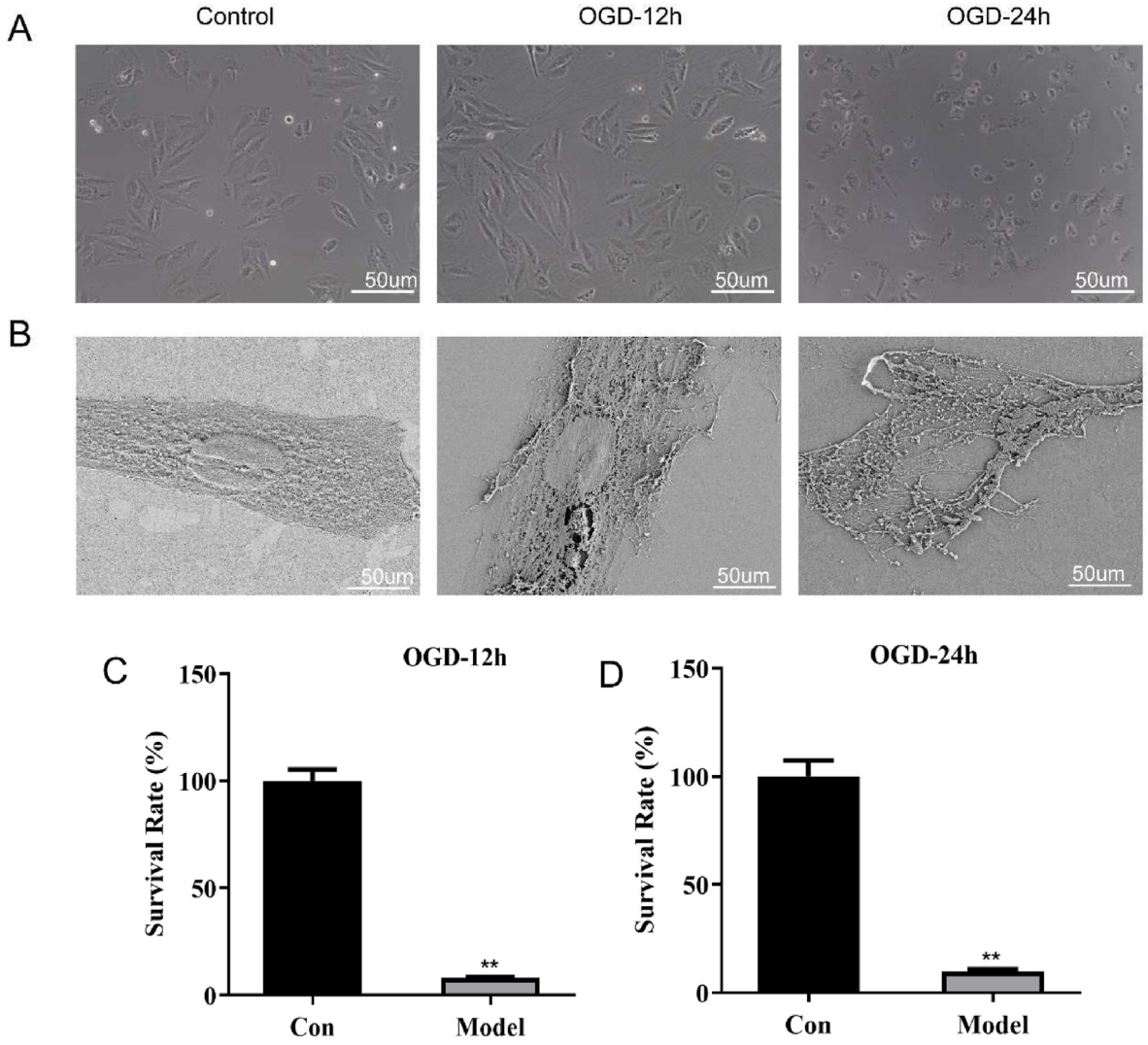

Fig. 1. Compared of OGD at 12 h or 24 h in H9c2. (**A**) Gross photographs of H9c2 morphology at different times (400 ×). (**B**) Scanning electron microscopy pictures of H9c2 at different times (400 ×). (**C**) Quantification of H9c2 survival rate was displayed at 12 h-OGD. (**D**) Quantification of H9c2 survival rate was exhibited at 24 h-OGD. Student's t-test was used for statistical analyses. Bars represent means ± SD; $^{**}P < 0.01$ vs. the control group.

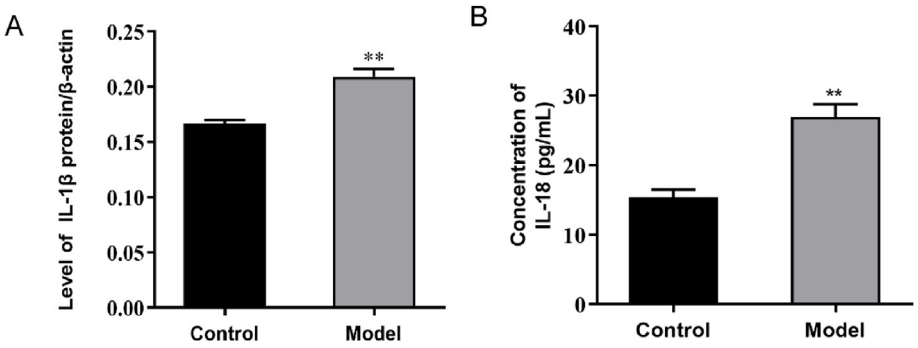

Fig. 2. IL-1β and IL-18 expression in H9c2 supernatant. (**A**) Quantification of IL-1β level was exhibited. (**B**) Quantification of IL-18 level was exhibited. Student's t-test was used for statistical analyses. Bars represent means ± SD; $^{**}P < 0.01$ vs. the control group.

12 h or 24 h of OGD, cell survival was significantly decreased compared with the control group ($P < 0.01$), and there was no significant difference in cell survival at 12 h or 24 h (Fig. 1C and D). Taking into consideration the damaging effect and cell morphology under the OGD, the 12 h OGD models were selected for in vitro.

3.8. The expression levels of IL-18 and IL-1β in the supernatant of OGD in H9c2 cells increased

IL-18 and IL-1β are two important inflammatory cytokines released after the occurrence of pyroptosis, which can reflect the degree of pyroptosis. To assess the levels of IL-18 and IL-1β released by H9c2 under the OGD, the amounts of two inflammatory cytokines were measured by 2 activity assay kits. As shown (Fig. 2): Compared with the control group, the secretion of IL-18 and IL-1β in the OGD group was significantly increased ($P < 0.01$).

3.9. Increased levels of pyroptosis-related proteins in the OGD of H9c2 cells

Ischemia and hypoxia are important inducers of pyroptosis. Under upstream OGD conditioning stimulation, whether H9c2 can

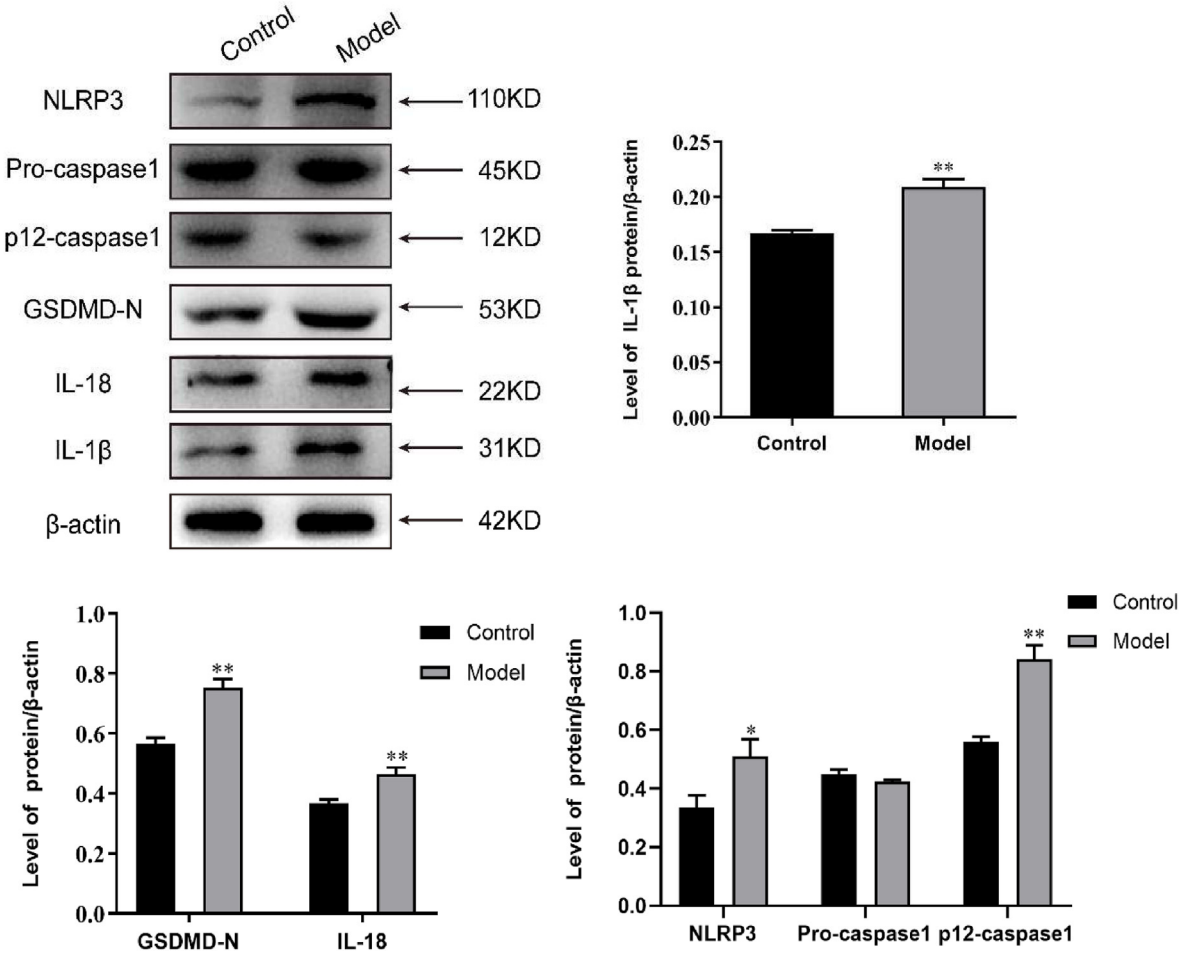

Fig. 3. Pyroptosis-related proteins levels in the OGD detected by western blotting. Student's t-test was used for statistical analyses. Bars represent means ± SD; $^{*}P < 0.05$, $^{**}P < 0.01$ vs. the control group.

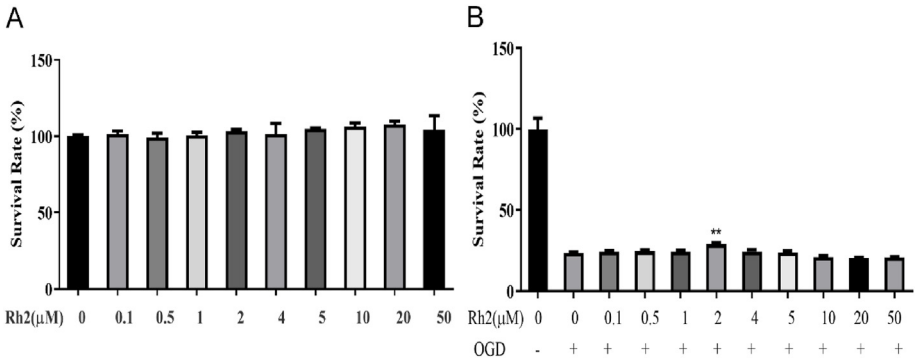

Fig. 4. Effect of Rh2 on H9c2 cytotoxicity. (**A**) CCK-8 was used to detect the toxicity of Rh2. (**B**) The optimal protective dose of Rh2 against H9c2 during the OGD. $P < 0.01$, compared with Model. One-way ANOVA test was used for statistical analyses. Bars represent means ± SD; $^{**}P < 0.01$ vs. the control group.

trigger pyroptosis, activate NLRP3 inflammasome activation, induce the activation of pyroptosis executive protein GSDMD-N, and rupture the cell membrane, release inflammatory factors to circulating tissues, and aggravate the progression of MI. The expression levels of pyroptosis-related proteins in the OGD were detected by western blotting. As shown (Fig. 3): The levels of proteins NLRP3, GSDMD-N, p12-caspase1, IL-1β, and IL-18 were significantly increased compared with the control group ($P < 0.01$ or $P < 0.05$).

3.9.1. 2 μM Rh2 effectively prevented H9c2 cells death

Rh2 was tested for toxicity to H9c2 by CCK-8. The results presented that 0.1–50 μM Rh2 did not inhibit H9c2 proliferation (Fig. 4A). In the OGD, 0.1–50 μM Rh2 was added, and the data showed that 2 μM Rh2 prevented significantly H9c2 death, compared with the model group ($P < 0.01$) (Fig. 4B).

3.10. Rh2 reduced IL-18 and IL-1β levels in the cell supernatant of H9c2 cells

IL-18 and IL-1β, as two specific inflammatory cytokines released after cell membrane damage during pyroptosis, can reflect the pyroptosis partially. The influence of Rh2 on the expression of IL-18 and IL-1β in the cell supernatant was shown (Fig. 5). Compared with the model group, when Rh2 was administrated, the accumulation of IL-18 was alleviated ($P < 0.05$), the activity of IL-1β significantly different ($P < 0.001$). The results pointed out that Rh2 can reduce the secretion of inflammatory cytokines by H9c2, which may be related to the inhibition of pyroptosis.

3.11. Rh2 down-regulated pyroptosis-related protein expression in H9c2 cells

As shown in the above results, Rh2 could lower the contents of IL-1β and IL-18 in the supernatant of H9c2, and whether the changes of the two inflammatory cytokines were directly related to the pyroptosis requires further clarification of the effects of Rh2 on leading involved proteins during the development of pyroptosis. The expression levels of related proteins were detected by Western blot (Fig. 6A), NLRP3 inflammasome was down-regulated with Rh2 treatment ($P < 0.05$) and inhibited the activation of p12-caspase1, a key protease during pyroptosis ($P < 0.01$), but had no significant effect on the pro-caspase1 ($P > 0.05$). We further evaluated pyroptosis signaling activity, GSDMD-N was significantly down-regulated, an essential protein of pyroptosis ($P < 0.01$), therefore, diminished the release of inflammatory cytokines IL-1β and IL-18 ($P < 0.01$). As a result, these data demonstrated that Rh2 can reduce the expression of pyroptosis-related proteins, alleviate the occurrence of inflammatory reactions, and protect cardiomyocytes.

3.12. Rh2 decreased HMGB1 protein expression in H9c2 cells

HMGB1, as a highly conserved nuclear protein, is released during inflammatory processes, such as programmed cell death, leading to a series of inflammatory cascades, which include pyroptosis. We selected the candidate drug-likeness Rh2 that can have a good binding ability to HMGB1 and play a role in myocardial protection. Additionally, whether Rh2 can change the expression of HMGB1. These results indicated (Fig. 6B) Rh2 decreased HMGB1 protein level ($P < 0.01$), restrained the occurrence of the inflammatory cascade, and influenced the process of pyroptosis.

4. Discussion

Although the integrated application of molecular docking and network pharmacology has attracted much attention, due to the non-uniform standards of numerous databases, the data of virtual screening cannot completely replace the experimental results, and it is necessary to combine more genomics technologies and

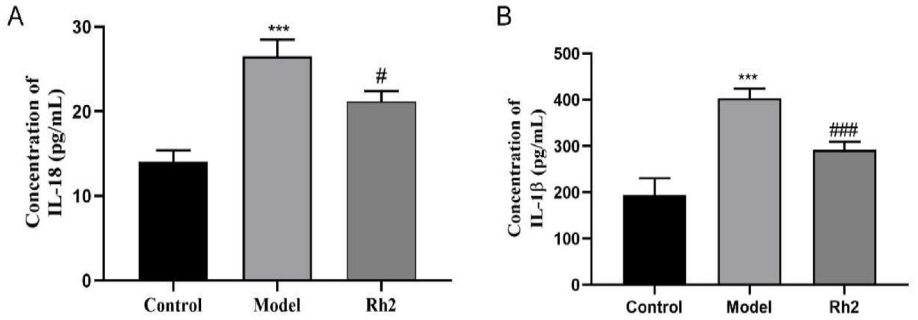

Fig. 5. Effect of Rh2 on IL-1β and IL-18 expression in the cell supernatant. (**A**) The effect of Rh2 on IL-18 levels. (**B**) Effect of Rh2 on IL-1β levels. One-way ANOVA test was used for statistical analyses. Bars represent means ± SD; $^{***}P < 0.001$, vs. the control group; $^{\#}P < 0.05$ *or* $^{\#\#\#}P < 0.001$, vs. the OGD group.

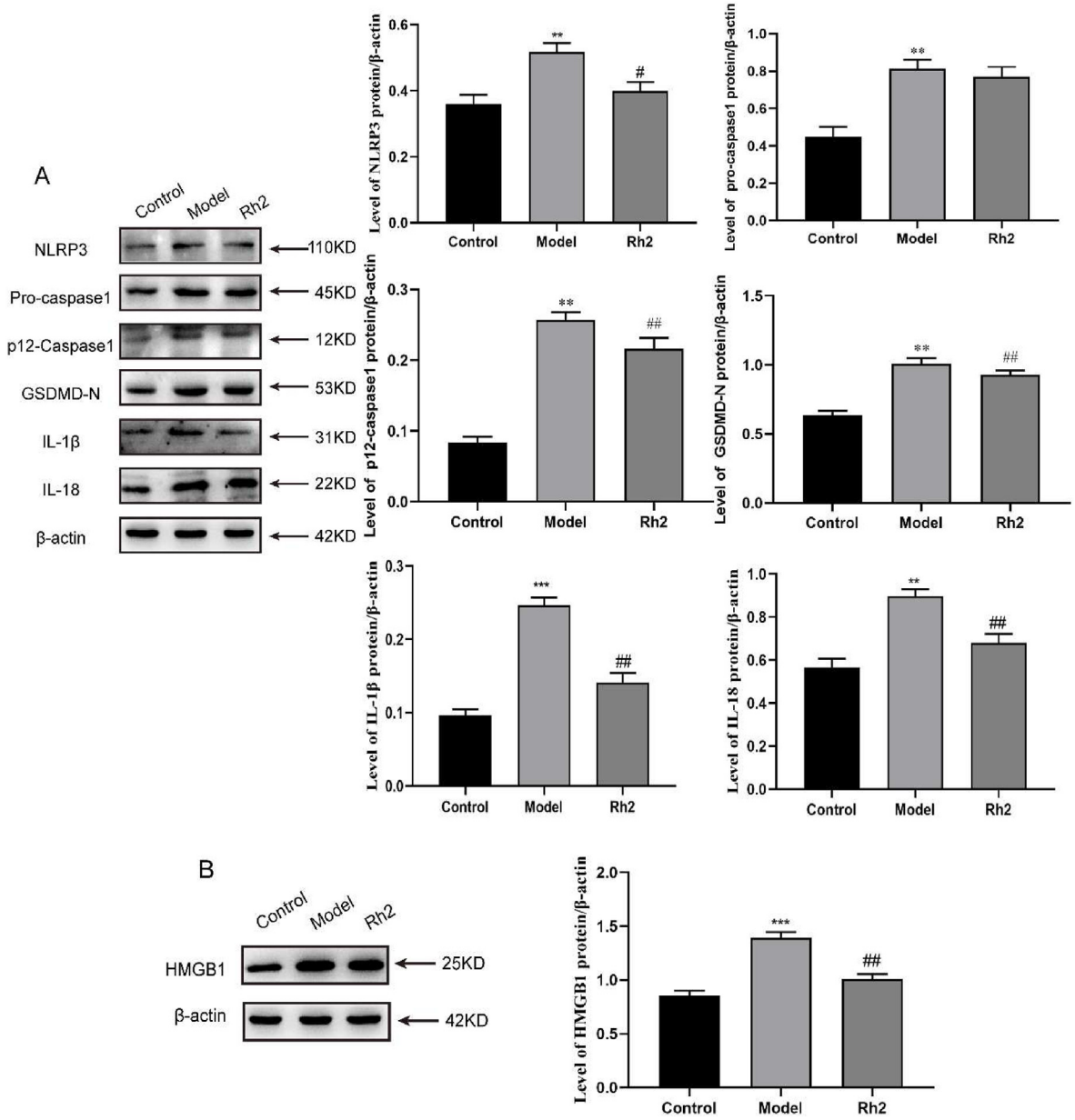

Fig. 6. Pyroptosis-related proteins were detected using Western blot analysis (**A**) The effect of Rh2 on pyroptosis-related proteins. (**B**) HMGB1 protein expression. One-way ANOVA test was used for statistical analyses. Bars represent means ± SD; $^{**}P < 0.05$ *or* $^{***}P < 0.01$, vs. the control group; $^{\#}P < 0.05$, $^{\#\#}P < 0.01$, vs. the OGD group.

experimentally verify its mechanism [31,32]. This comprehensive bioinformatic analysis provided 29, 95, 96, and 34 active ingredients of *Hedysarum Multijugum Maxim*, *Panax Notoginseng*, *Radix Salviae,* and *Dalbergia Odorifera* through the TCMSP database, respectively, and predicted potential targets of active compounds via the TCMSP platform, mapping a total of 29 identical targets of compounds. The Genecards database was applied to screen likely targets associated with MI and pyroptosis, and 5 typical workable target proteins, CASP1, HMGB1, PARP1, BCL2, and EGFR, were acquired by topological analysis. ADME parameters can be acted as a meaningful standard for drug candidates, coupled with OB, DL, and HLcharacteristics, to extract 7 top candidate active components, sinophenol, mistletoe, luteolin, dehydrobaicalein IIA, β-sitosterol, Rh2, and ginseng epoxyethinol, which were also concerned by the hemodynamics of patients with myocardial infarction, and the DH of β-sitosterol and Rh2 is exceedingly short at 5.36 h and 11.08 h, respectively. These findings suggested that β-sitosterol and Rh2 were more appropriate as drug candidates for the therapeutic potential of MI. Molecular docking validation of the target protein with the 2 drug candidates practicing Autodock software revealed that Rh2 had stable binding energy to HMGB1.

Rh2 is derived from *Panax Notoginseng* in QSYQ Pills. With the profound study of the pharmacodynamic components of TCM in recent years, the research of *Panax Notoginseng* has become more and more refined [33]. Having been ascertained that saponins are the main active components of *Panax Notoginseng*, mainly including *Panax Notoginseng Saponins* R1-R6, ginsenosides Rb, Rd, Re, Rg1, Rg2, as well as some brass and sterol rare components [34,35]. Ginsenoside Rh2 has gained more and more attention as a rare saponin ingredient in *Panax Notoginseng Saponins* [36]. Although the relative content is lower, its chemical composition is corresponding to ginseng, a valuable Chinese medicinal herb. Therefore, Rh2 as prominent drug research and medicinal resource utilization are actively carried out, and some single drug varieties

have been fortunately marketed, such as notoginseng powder and notoginsenoside injection, which are applied clinically.

Rh2, as a secondary ginsenoside, can be taken as an alternative component of ginseng and play a protective myocardial role in diabetic myocardial injury rats. The researcher injected streptozocin-induced diabetic rats to form a diabetic cardiomyopathy model, and then detected the level of superoxide dismutase (SOD), glutathione peroxidase (GSH-Px), and reactive oxygen species (ROS) in serum and heart tissue. Their findings displayed that Rh2 could improve cardiac function, and the mechanism may be linked to reducing ROS overproduction in tissues, upregulating SOD expression. Hence, Rh2 had a strong antioxidant capacity in vivo and prevent cardiomyocyte injury [37]. At the same time, screened the main active components of *Panax Notoginseng* in the intervention of osteonecrosis of the femoral head by network pharmacology, and 8 active components including mistletoe and ginsenoside Rh2 and 98 disease targets were selected by constructing a main component-disease target network, it was clarified that quercetin and Rh2 in *Panax Notoginseng* may be potential targets for the treatment of osteonecrosis of the femoral head [38]. Additionally, Rh2 could inhibit the expression of IL-6, IL-1β, and tumor necrosis factor (TNF-α) and increase the release of IL-10 in LPS-induced mouse mononuclear macrophages (RAW264.7) in a dose-dependent manner, indicating that Rh2 regulated the pro-inflammatory/anti-inflammatory balance [39]. Angiogenesis and coagulation dysfunction are the key points in the pathological process of cardiovascular diseases, previous researches have shown that Rh2 may prolong prothrombin time (PT) and activated partial thromboplastin time (APTT) and present an anticoagulant mechanism, furthermore, Rh2 could change the expression of vascular endothelial growth factor (VEGF) and receptor-related binding protein, alter the activation of downstream AKT and extracellular signal-regulated kinase (ERK) pathways, and increase cell migration ability and angiogenesis [40].

Pyroptosis is a form of programmed cell death. Activated caspase-1 promotes the cutting activation and translocation of GSDMD-N [41,42], leads to change in cell membrane permeability [43], releases IL-1β and IL-18, accelerates myocardial injury, and finally forms a vicious cycle of "inflammatory activation-pyroptosis-inflammatory response". Therefore, the pyroptosis-inflammatory response may be a critical strategy to inhibit the inflammatory response after MI. HMGB1 is a nuclear protein with high content, and previous studies have demonstrated that it is involved in the progression of a variety of inflammatory diseases [44,45]. Alternatively, the NLRP3 inflammasome accelerates HMGB1 release from the nucleus [46], further mediating the inflammatory response and activating downstream inflammation-related proteins [47]. HMGB1 is also a significant downstream pathway of pyroptosis [48]. Through our study, network pharmacology, and molecular docking analysis of QSYQ pills, HMGB1 was obtained to be an important target protein of MI-pyroptosis-QSYQ, which was also in proportion to numerous studies on the role of HMGB1 in pyroptosis.

To evaluate the therapeutic effect of Rh2 on MI, the construction of the OGD model in vitro can simulate the pathological process. At 12 h-OGD in H9c2, multiple pores were formed or even ruptured on the cell membrane surface, which was consistent with the characteristics of pyroptosis damage. The data in this paper showed that the OGD model induced NLRP3 inflammasome overproduction in vitro, causing an increase in myocardial caspase-1 production. Caspase-1 can attack activation of pyroptosis-executing HMGB1, and enlarged release of IL-18 and IL-1β cytokines. After Rh2 treatment, 2 μM Rh2 prevented OGD-induced H9c2 death and reduced IL-18 and IL-1β levels in the supernatant of OGD, which may play a role in protecting H9c2 injury by alleviating the expression of pyroptosis-related proteins, inhibiting the activation of pyroptosis, down-regulating the activation of inflammatory. When cells are stimulated by external conditions, HMGB1 is released from the damaged nucleus to the outside of the nucleus in a simple diffusion manner, activating the NLRP3 inflammasome by binding endogenous pattern recognition receptors and subsequently activating caspase-1. GSDMD is a substrate of caspase protein, and caspase-1 can specifically cleave GSDMD after activation, and the *N*-terminal protein of the broken GSDMD protein has punching activity and can insert into the cell membrane to form pore, which triggers pyroptosis. In this study, we further confirmed that Rh2 can reduce the extracellular release of HMGB1, which in turn inhibits the HMGB1-dependent caspase-1/GSDMD signaling axis, thereby alleviating cardiomyocyte anxiety.

Our study had several limitations. Firstly, we failed to further clarify the role of Rh2 in vivo in MI. Secondly, we did not examine the effect of more doses of Rh2 and myocardial protection. Thirdly, there are classical and non-classical pathways in the development of pyroptosis, and caspase-11, caspase-3, and caspase-5 also play an important role. The future work direction will be to carry out clinical research on Rh2 as a candidate new drug for cardiovascular diseases.

5. Conclusion

We propose that Rh2 of QSYQ can protect cardiomyocytes partially by ameliorating pyroptosis, which seems to have a new insight regarding the therapeutic potential for MI.

Availability of data and materials

The original contributions presented in the study are included in the article/Supplementary Material. Further inquiries can be directed to the corresponding authors.

Author contributions

ZW-Q was in charge of doing experimental design, basic experiments, data statistics, and writing articles. ZP-Y, YY-W, and NJ were in charge of doing the basic experiments, including pathological analysis. JP-Z was in charge of directing the experimental work and reviewing this article. XY-Y and AZ were in charge of doing the network pharmacology and molecular docking analysis. ML and FQ-X revised the manuscript. All authors contributed to the article and approved the submitted version.

Funding

This study was supported by the National Natural Science Foundation of China (Grant No. 81804046, 81,774,232).

Appendix A. Supplementary data

Supplementary data to this article can be found online at https://doi.org/10.1016/j.jgr.2022.03.003.

References

[1] Jiao X, Jin X, Ma Y, Yang Y, Li J, Liang L, Liu R, Li Z. A comprehensive application: molecular docking and network pharmacology for the prediction of bioactive constituents and elucidation of mechanisms of action in component-based Chinese medicine. Comput Biol Chem 2021;90:107402.

[2] Tsai FJ, Li TM, Cheng CF, Wu YC, Lai CH, Ho TJ, Liu X, Tsang H, Lin TH, Liao CC, et al. Effects of Chinese herbal medicine on hyperlipidemia and the risk of cardiovascular disease in HIV-infected patients in Taiwan. J Ethnopharmacol 2018;219:71–80.

[3] De Las Rivas J, Bonavides-Martínez C, Campos-Laborie FJ. Bioinformatics in Latin America and SoIBio impact, a tale of spin-off and expansion around genomes and protein structures. Briefings Bioinf 2019;20:390–7.
[4] Pradeepkiran JA, Reddy PH. Structure based design and molecular docking studies for phosphorylated tau inhibitors in Alzheimer's disease. Cells 2019;8.
[5] Saikia S, Bordoloi M. Molecular docking: challenges, advances and its use in drug discovery perspective. Curr Drug Targets 2019;20:501–21.
[6] Morris GM, Lim-Wilby M. Molecular docking. Methods Mol Biol 2008;443:365–82.
[7] Kitchen DB, Decornez H, Furr JR, Bajorath J. Docking and scoring in virtual screening for drug discovery: methods and applications. Nat Rev Drug Discov 2004;3:935–49.
[8] Kumar A, Tiwari A, Sharma A. Changing paradigm from one target one ligand towards multi-target directed ligand design for key drug targets of Alzheimer disease: an important role of in silico methods in multi-target directed ligands design. Curr Neuropharmacol 2018;16:726–39.
[9] Chen L, Du J, Dai Q, Zhang H, Pang W, Hu J. Prediction of anti-tumor chemical probes of a traditional Chinese medicine formula by HPLC fingerprinting combined with molecular docking. Eur J Med Chem 2014;83:294–306.
[10] Hopkins AL. Network pharmacology. Nat Biotechnol 2007;25:1110–1.
[11] Shin SY, Müller AK, Verma N, Lev S, Nguyen LK. Systems modelling of the EGFR-PYK2-c-Met interaction network predicts and prioritizes synergistic drug combinations for triple-negative breast cancer. PLoS Comput Biol 2018;14:e1006192.
[12] Li M, Qi Z, Zhang J, Zhu K, Wang Y. Effect and mechanism of Si-Miao-Yong-An on Vasa Vasorum remodeling in ApoE(-/-) mice with atherosclerosis vulnerable plague. Front Pharmacol 2021;12:634611.
[13] Qi Z, Li M, Zhu K, Zhang J. Si-Miao-Yong-An on promoting the maturation of Vasa Vasorum and stabilizing atherosclerotic plaque in ApoE(-/-) mice: an experimental study. Biomed Pharmacother 2019;114:108785.
[14] Zhang Y, Shi P, Yao H, Shao Q, Fan X. Metabolite profiling and pharmacokinetics of herbal compounds following oral administration of a cardiovascular multi-herb medicine (Qishen yiqi pills) in rats. Curr Drug Metabol 2012;13:510–23.
[15] Huang Y, Zhang K, Liu M, Su J, Qin X, Wang X, Zhang J, Li S, Fan G. An herbal preparation ameliorates heart failure with preserved ejection fraction by alleviating microvascular endothelial inflammation and activating NO-cGMP-PKG pathway. Phytomedicine 2021;91:153633.
[16] Hou YZ, Wang S, Zhao ZQ, Wang XL, Li B, Soh SB, Mao JY. Clinical assessment of complementary treatment with Qishen Yiqi dripping pills on ischemic heart failure: study protocol for a randomized, double-blind, multicenter, placebo-controlled trial (CACT-IHF). Trials 2013;14:138.
[17] Lv S, Yuan P, Dong J, Lu C, Li M, Qu F, Zhu Y, Yuan Z, Zhang J. QiShenYiQi pill improves the reparative myocardial fibrosis by regulating autophagy. J Cell Mol Med 2020;24:11283–93.
[18] An N, Gao Y, Si Z, Zhang H, Wang L, Tian C, Yuan M, Yang X, Li X, Shang H, et al. Regulatory mechanisms of the NLRP3 inflammasome, a novel immune-inflammatory marker in cardiovascular diseases. Front Immunol 2019;10:1592.
[19] Yan Z, Qi Z, Yang X, Ji N, Wang Y, Shi Q, Li M, Zhang J, Zhu Y. The NLRP3 inflammasome: multiple activation pathways and its role in primary cells during ventricular remodeling. J Cell Physiol 2021;236:5547–63.
[20] Lv S, Yuan P, Lu C, Dong J, Li M, Qu F, Zhu Y, Zhang J. QiShenYiQi pill activates autophagy to attenuate reactive myocardial fibrosis via the PI3K/AKT/mTOR pathway. Aging 2021;13:5525–38.
[21] Ru J, Li P, Wang J, Zhou W, Li B, Huang C, Li P, Guo Z, Tao W, Yang Y, et al. TCMSP: a database of systems pharmacology for drug discovery from herbal medicines. J Cheminf 2014;6:13.
[22] Su X, Kong L, Lei X, Hu L, Ye M, Zou H. Biological fingerprinting analysis of traditional Chinese medicines with targeting ADME/Tox property for screening of bioactive compounds by chromatographic and MS methods. Mini Rev Med Chem 2007;7:87–98.
[23] Tao W, Xu X, Wang X, Li B, Wang Y, Li Y, Yang L. Network pharmacology-based prediction of the active ingredients and potential targets of Chinese herbal Radix Curcumae formula for application to cardiovascular disease. J Ethnopharmacol 2013;145:1–10.
[24] Breuza L, Poux S, Estreicher A, Famiglietti ML, Magrane M, Tognolli M, Bridge A, Baratin D, Redaschi N. The UniProtKB guide to the human proteome, vol. 2016. Oxford: Database; 2016.
[25] Shannon P, Markiel A, Ozier O, Baliga NS, Wang JT, Ramage D, Amin N, Schwikowski B, Ideker T. Cytoscape: a software environment for integrated models of biomolecular interaction networks. Genome Res 2003;13:2498–504.
[26] Paolacci S, Precone V, Acquaviva F, Chiurazzi P, Fulcheri E, Pinelli M, Buffelli F, Michelini S, Herbst KL, Unfer V, et al. Genetics of lipedema: new perspectives on genetic research and molecular diagnoses. Eur Rev Med Pharmacol Sci 2019;23:5581–94.
[27] Taha KF, Khalil M, Abubakr MS, Shawky E. Identifying cancer-related molecular targets of Nandina domestica Thunb. by network pharmacology-based analysis in combination with chemical profiling and molecular docking studies. J Ethnopharmacol 2020;249:112413.
[28] Daga PR, Polgar WE, Zaveri NT. Structure-based virtual screening of the nociceptin receptor: hybrid docking and shape-based approaches for improved hit identification. J Chem Inf Model 2014;54:2732–43.
[29] Trott O, Olson AJ. AutoDock Vina: improving the speed and accuracy of docking with a new scoring function, efficient optimization, and multithreading. J Comput Chem 2010;31:455–61.
[30] Gaillard T. Evaluation of AutoDock and AutoDock vina on the CASF-2013 benchmark. J Chem Inf Model 2018;58:1697–706.
[31] Yadav BS, Tripathi V. Recent advances in the system biology-based target identification and drug discovery. Curr Top Med Chem 2018;18:1737–44.
[32] Kibble M, Saarinen N, Tang J, Wennerberg K, Mäkelä S, Aittokallio T. Network pharmacology applications to map the unexplored target space and therapeutic potential of natural products. Nat Prod Rep 2015;32:1249–66.
[33] Ni KL, Han LF, Zhao N, He TT, Chai JH. A new dammarane-tye triterpenoid saponin from roots of Panax notoginseng. Chin Tradit Herb Drugs 2019;50:2273–8.
[34] Huang JW, Li CJ, Yang JZ, Ma J, Zang DM. Chemical constituents from leaves of Panax notoginseng and anti-oxidant activity. Chin Tradit Herb Drugs 2017;48:4381–6.
[35] Xing N, Peng DH, Zhang ZH, Zhang ZD, Kuan HX, Wang QH. Progress in Research on Effect of Processing on Chemical Constituents and Pharmacological Effect of Notoginseng Radix et Rhizoma. Chin J Exp Tradit Med Form 2020;26:210–27.
[36] Li GM, Li Y. Research status of pharmacological effects of ginsenosides. Chin J Clin Pharmacol 2020;36:1024–7.
[37] Qu M, Wang N, Dong ZH. Effects of ginsenoside Rh2 on myocardial oxidative stress in diabetic rats. J Beihua Univ Nat Sci 2015;16:741–7.
[38] Nong J, Zeng P, Li J, Liu JF, Li JY. Immunoinflammatory mechanism of Panax notoginseng in the treatment of osteonecrosis of the femoral head based on network pharmacology. Chin J Tissue Eng Res 2020;24:4613–9.
[39] Wu YX, Wu LP, Hu CY, Wan ZB, Li KB, Kim TW. Effect of sanggenon B from cortex mori on lipopolysaccharide-induced inflammatory response in RAW264. Nat Prod Res Dev 2018;30:1132–7.
[40] Zhang XP, Li KR, Yu Q, Yao MD, Ge HM, Li XM, Jiang Q, Yao J, Cao C. Ginsenoside Rh2 inhibits vascular endothelial growth factor-induced corneal neovascularization. Faseb J 2018;32:3782–91.
[41] Platnich JM, Muruve DA. NOD-like receptors and inflammasomes: a review of their canonical and non-canonical signaling pathways. Arch Biochem Biophys 2019;670:4–14.
[42] Cao H, Liang J, Liu J, He Y, Ke Y, Sun Y, Jiang S, Lin J. Novel effects of combination therapy through inhibition of caspase-1/gasdermin D induced-pyroptosis in lupus nephritis. Front Immunol 2021;12:720877.
[43] Chen S, Mei S, Luo Y, Wu H, Zhang J, Zhu J. Gasdermin family: a promising therapeutic target for stroke. Transl Stroke Res 2018;9:555–63.
[44] Yang H, Antoine DJ, Andersson U, Tracey KJ. The many faces of HMGB1: molecular structure-functional activity in inflammation, apoptosis, and chemotaxis. J Leukoc Biol 2013;93:865–73.
[45] Venereau E, De Leo F, Mezzapelle R, Careccia G, Musco G, Bianchi ME. HMGB1 as biomarker and drug target. Pharmacol Res 2016;111:534–44.
[46] Jessop F, Holian A. Extracellular HMGB1 regulates multi-walled carbon nanotube-induced inflammation in vivo. Nanotoxicology 2015;9:365–72.
[47] Xiao Y, Ding L, Yin S, Huang Z, Zhang L, Mei W, Wu P, Wang P, Pan K. Relationship between the pyroptosis of fibroblast-like synoviocytes and HMGB1 secretion in knee osteoarthritis. Mol Med Rep 2021;23.
[48] Chi W, Chen H, Li F, Zhu Y, Yin W, Zhuo Y. HMGB1 promotes the activation of NLRP3 and caspase-8 inflammasomes via NF-κB pathway in acute glaucoma. J Neuroinflammation 2015;12:137.